Available online at www.sciencedirect.com
SCIENCE DIRECT®
International Journal of Mass Spectrometry 244 (2005) 76–83
International Journal of Mass Spectrometry
www.elsevier.com/locate/ijms

Electron impact ionization of beryllium isoelectronic ions

M.Alfaz Uddin[a,*], A.K.F. Haque[a], M.S. Mahbub[a], K.R. Karim[b], A.K. Basak[a], B.C. Saha[c]

[a] *Department of Physics, University of Rajshahi, Matihar, Rajshahi 6205, Bangladesh*
[b] *Department of Physics, Illinois State University, Normal, IL 61790, USA*
[c] *Department of Physics, Florida A & M University, Tallahassee, FL 32307, USA*

Received 20 March 2005; received in revised form 4 May 2005; accepted 4 May 2005
Available online 14 June 2005

Abstract

The electron impact single ionization cross-sections on the Be, B^+, C^{2+}, N^{3+}, O^{4+}, Ne^{6+}, Fe^{22+} and U^{88+} atomic targets, in the beryllium isoelectronic sequence (BIS), are calculated using the modified versions of simplified improved binary-encounter dipole model (siBED) [W.M. Huo, Phys. Rev. A 64 (2001) 042719]. The modified models, QIBED (with the ionic correction) and RQIBED (with both the ionic and relativistic corrections) [M.A. Uddin, A.K.F. Haque, A.K. Basak, B.C. Saha, Phys. Rev. A 70 (2004) 032706], are found to provide an excellent description of the experimental data for all the targets in BIS with the same generic values of the two parameters d_1 and d_2 in the models. The RQIBED results describe satisfactorily the assessed data of Be and its predictions for U^{88+} account for well the experimental K-shell ionization data of Sn, with almost the same properties of the ionized orbit concerned, even up to around 2 MeV.

PACS: 34.80.Dp

Keywords: Cross-sections; Electron-impact ionization; Beryllium-like ions

1. Introduction

The electron impact (EI) ionization of atoms and ions is a topic, which has had the attention of researchers during the last 100 years from the early days of modern physics. Nevertheless, the interest in this field has not diminished during the last decade. An important driving force for these studies is the field of applications. The ionization cross-sections are essential in modeling and understanding the behavior of hot plasmas in fusion research and astrophysical objects, ionization mass spectrometry, etc.

In recent years, various quantal methods have been developed for generating accurate cross-sections. However, they are confined to simple atomic and ionic targets [1–19]. Although these rigorous calculations are arduous, the performance of these methods in describing the experimental data is rather quite limited. The applied area requires a rapid generation of reasonably accurate (up to 30%) cross-sections over a wide range of incident energies and targets including the exotic ones as well as in the metastable states of targets. Practitioners, therefore, search for simple models, which can provide sufficiently accurate data easily.

Various simple approaches, namely the classical theory of Thomson [20], the empirical formula of Lotz [21,22], the classical model of Gryzinski [23] and the empirical model of Bernshtam et al. [24], have been evolved. The model of Deutsch and Märk (DM) [25] has been applied to neutral atoms and molecules [26–32]. A good review of various theoretical studies on the EI ionization is provided in [25,33,34]. Amongst other successful theoretical models, those of Kim and Rudd [35], Rost [36], Saksena et al. [37], and Khare et al. [38] deserve mentioning. The binary-encounter dipole (BED) model of Kim and Rudd [35] has enjoyed much applications in molecular targets [39–43] than their atomic counterparts.

In the BED model, the Mott cross-section has been modified and combined with the leading dipole-term of the Bethe cross-section to account for the dipole interaction (soft collision), characteristic of the bound electrons. The Mott as well

* Corresponding author.
E-mail address: alfazphy@yahoo.com, mauddin@ru.ac.bd (M. Alfaz Uddin).

1387-3806/$ – see front matter © 2005 Elsevier B.V. All rights reserved.
doi:10.1016/j.ijms.2005.05.002

as the Bethe cross-section has the kinetic energy of the incident electron T as the first denominator. The incident electron is attracted by the positive charge of the target nucleus and this process enhances the kinetic energy by the so-called *acceleration term*, $U + I$ (U and I being, respectively, the kinetic and binding energies of target electron). In the BED model, Burgess [44] replaced the first denominator T by $T + U + I$ and this simple prescription modifies the T-dependent correlation term between the incident and bound electrons. In spite of the considerable success of the BED model and its simpler versions, there remain some anomalies in its structure as noted in [45].

The improved binary-encounter dipole (iBED) model [45] replaces the Bethe cross-section term with a simple two-parameter dependent Born term. It thus removed the ambiguity associated with the Bethe term in the BED model and its versions. The two parameters of iBED are species dependent and are related to the nature of the charge distribution in the bonding region of the molecules. Nevertheless, Huo [45] derived a simplified version of iBED (siBED), where the two parameters can assume generic values. Uddin et al. [46] applied this siBED model to the atomic targets in the helium isoelectronic sequence covering a wide range of atomic number Z on a broad range of electron incident energies extending to the relativistic domain. It has been observed that siBED works well with a neutral atomic target like He but it needs modifications in terms of the ionic and relativistic effects. For the ionic targets these modifications are essential as demonstrated earlier in [46]. The ionic correction is incorporated by including the charge parameter q of the target in the Burgess denominator [47,48] of the Mott part of the siBED model. This has led to the development of the QIBED (siBED with ionic correction) model [46]. The inclusion of both the ionic and relativistic effects has produced the RQIBED model [46].

Systematic studies along an isoelectronic sequence of the atoms and ions are desirable to aid the continuing efforts in developing model formulas. In particular, after the stupendous success of RQIBED in describing the EI ionization data of all the helium isoelectronic targets [46] with a constant set of values for the two parameters d_1 and d_2, it naturally poses the question: *whether or not these same parameter values can generate an identical success for other isoelectronic targets*. When the values of the two parameters commensurate with the electronic structure of the target are determined, RQIBED does not remain any more a fitting formula but behaves like a parameter-free model. With this in view, our objective in the present work is to examine both the QIBED and RQIBED models on the targets of the beryllium sequence. We would like to emphasize here that the two parameters d_1 and d_2 in the QIBED and RQIBED models are dependent mainly on the electronic structure of the target but independent of the projectile energy in conformity with our earlier studies [46,49]. Similar observations were also made by Huo [45] for molecular targets. We use the available experimental EI ionization cross-sections for adjusting the two parameters d_1 and d_2. The derived set of these values are then held constant in both the QIBED and RQIBED calculations for the atomic Be and the ionic targets, B^+, C^{2+}, N^{3+}, O^{4+}, Ne^{6+}, Fe^{22+} and U^{88+}. We then compare our findings with other theoretical calculations, such as the distorted-wave Born approximation with R-matrix (DWBARM) of Laghdas et al. [16], the no-exchange distorted-wave Coulomb–Born approximation (NXDCB) of Moores [50], the distorted-wave Coulomb–Born approximation with exchange (DCBX) [51], the analytic fit to the distorted-wave Born-exchange approximation (DWBX) of Younger [52], the orthogonalized Born–Oppenheimer approximation (OBO) [53] and the relativistic distorted wave Born approximation (RDWBA) [54]. To adjudge the performance of QIBED and RQIBED, we also calculate the cross-sections from the parent siBED model, the empirical model of Bernshtam et al. (henceforth referred to as BRY) [24], the MBED model [55] and the assessed data of Bell et al. [56].

In Section 2, we present a brief description of the siBED, QIBED and RQIBED models. Discussions on the results are furnished in Section 3 and a brief summary of the conclusions is listed in Section 4.

2. Outline of the models

The cross-section in the QIBED model [46] is given by

$$\sigma_{\mathrm{QIBED}} = \sigma^{Q}_{\mathrm{Mott}} + \sigma^{Q}_{\mathrm{Born}}, \tag{1}$$

where $\sigma^{Q}_{\mathrm{Mott}}$ is the modified Mott cross-section [45]

$$\sigma^{Q}_{\mathrm{Mott}} = S^{Q} H \tag{2}$$

with

$$H = \left[\frac{k_0^2 - \alpha_0^2}{k_0^2 \alpha_0^2} - \frac{\ln(k_0^2/\alpha_0^2)}{k_0^2 + \alpha_0^2} \right], \tag{3}$$

and

$$S^{Q} = \frac{4\pi N_0}{k_0^2 + (k_{\mathrm{b}}^2 + \alpha_0^2)/(q+1)}, \tag{4}$$

and $\sigma^{Q}_{\mathrm{Born}}$ is the dipole-Born cross-section [45] given by

$$\sigma^{Q}_{\mathrm{Born}} = F^{Q} G \tag{5}$$

with

$$F^{Q} = \frac{64\alpha_0^3 N_0}{k_0^2}, \tag{6}$$

$$G = \int_0^{(k_0^2-\alpha_0^2)/2} k_{\mathrm{p}} (k_{\mathrm{p}}^2 + \alpha_0^2)^2 \, \mathrm{d}E_{\mathrm{p}} \times \int_{K_{\min}}^{K_{\max}} \frac{1 + d_1 t + d_2 t^2}{K[(K+k_{\mathrm{p}})^2 + \alpha_0^2]^3 [(K-k_{\mathrm{p}})^2 + \alpha_0^2]^3} \, \mathrm{d}K, \tag{7}$$

and

$$t = \frac{K^4}{[(K+k_p)^2+\alpha_0^2][(K-k_p)^2+\alpha_0^2]}. \quad (8)$$

Here, $T = k_0^2/2$ is the energy of the incident electron; $U = k_b^2/2$, the kinetic energy of the bound electron; $I = \alpha_0^2/2$, the binding energy of the target electron and $E_p = k_p^2/2$, the energy of the ejected electron with α_0 having the dimension of momentum in the atomic unit [45]. $\mathbf{K} = \mathbf{k}_0 - \mathbf{k}_1$ denotes the momentum transfer vector with $\mathbf{k}_1$ representing the momentum of the electron after a collision in the atomic unit. The maximum and minimum values of K are given in [57]. N_0 is the number of electrons in the orbit considered and q denotes the ionic charge of the target.

The Mott part σ_{Mott}^{Q} in (1) represents the cross-section arising from the direct ($l = 0$) interaction, while the Born part σ_{Born}^{Q} originates from the dipole ($l = 1$) interaction. The first term of H in (3) embodies the direct and exchange contributions, and the second one, the logarithmic term, denotes the interference of the two. The denominator of S^Q in (4) replaces the incident energy by an effective energy in the binary-encounter model, modified with the ionic factor $(q + 1)$. The first term in the numerator $(1 + d_1 t + d_2 t^2)$ in (7) represents the contribution from the long-range part of the dipole interaction, and the terms involving the parameters d_1 and d_2 denote the effect from the short-ranged shielded part of the dipole interaction (see [45]). The parameters d_1 and d_2 have dependence on the electronic structure of the target. They can conveniently be evaluated by comparing of the calculated cross-sections with the experimental data.

In modifying the siBED model [45] for the relativistic effect, we retain the original structure of the interaction matrix element and infuse the relativistic components through the prefactors of S^Q in (4) and F^Q in (6) following closely the work of Deutsch's group [27,32], Casnati et al. [58] and Hombourger [59]. This simple prescription for the RQIBED model has been applied with a considerable success not only for the He isoelectronic sequence [46] but also for the K-shell ionization of atoms [49]. In the RQIBED model, the expression for the EI ionization cross-section has been shown [46] to have the form:

$$\sigma_{\text{RQIBED}} = \sigma_{\text{Mott}}^{R} + \sigma_{\text{Born}}^{R}, \quad (9)$$

where

$$\sigma_{\text{Mott}}^{R} = S^R H, \quad (10)$$

$$\sigma_{\text{Born}}^{R} = F^R G, \quad (11)$$

$$S^R = \frac{4\pi N_0 \alpha^2}{\beta_t^2 + (\beta_b^2 + \beta_a^2)/(q+1)}, \quad (12)$$

$$F^R = \frac{64\beta_a^3 N_0}{\alpha \beta_t^2}. \quad (13)$$

Using m as the mass of the electron, c as the velocity of light in the free space and α as the fine structure constant, the quantities β_t, β_b and β_a in (12) and (13) are defined in terms of $t' = k_0^2/2mc^2$, $b' = k_b^2/2mc^2$ and $a' = \alpha_0^2/2mc^2$, respectively, as

$$\beta_t^2 = 1 - \frac{1}{(1+t')^2}, \quad (14)$$

$$\beta_b^2 = 1 - \frac{1}{(1+b')^2}, \quad (15)$$

and

$$\beta_a^2 = 1 - \frac{1}{(1+a')^2}. \quad (16)$$

3. Results and discussion

For the neutral targets, we used the ionization potential given by Desclaux [60]. The kinetic energy of the bound electron of all targets and the ionization potentials of the ionic targets are calculated using the Dirac–Hartree–Fock code [61]. Using the 64-point Gauss–Legendre rule [62] the two-dimensional integrations over K and E_p in the siBED, QIBED and RQIBED calculations are carried out numerically. The two parameters, d_1 and d_2, are determined by the least-square fitting code MINUIT [63]. As pointed out in [45], the value of d_1 determines the cross-section peak. The value of $d_1 = 0.0$ in the siBED model [45] for the neutral molecules, which has been found good for the helium isoelectronic targets, is also found appropriate to all the targets in this study. The parameter d_2 mainly governs the high energy behavior of the cross-sections. It is found that the values of d_2 in the range 0.0–0.05 along with $d_1 = 0.0$ provide close fit to the data. Fig. 1 depicts the calculated cross-sections, summed over all orbits, in the typical case of the N^{3+} target for the different values of d_2 using the RQIBED model. Since the relativistic effect is negligibly small in the energy range, especially for the light atomic targets considered herein, both the QIBED and RQIBED results agree nicely. In this figure, the heavy solid, shaded, short-dashed and light solid curves labelled, respectively, by RQIBED00, RQIBED01, RQIBED03 and RQIBED05 representing the calculations with $d_2 = 0.0$, 0.01, 0.03 and 0.05, while keeping d_1 fixed at 0.0 for all cases. It is clear from the figure that for $d_2 \geq 0.01$, the cross-sections diverge at higher energies. The set of values $d_1 = d_2 = 0.0$ gives not only the required convergence in cross-sections at higher energies, but also produce satisfactory fits to the experimental data for all the targets, as we will view later. These values are held fixed throughout the subsequent calculations.

Figs. 2–9 present our results from the siBED, QIBED and RQIBED models using $d_1 = d_2 = 0.0$ along with the experimental and other theoretical cross-sections. For the case of U^{88+}, the EI cross-sections are considered only from the 2s orbit while for all other targets in this study these represent the summed cross-sections over all orbits. As noted earlier, the BRY and MBED cross-sections are also calculated in the present study for comparison.

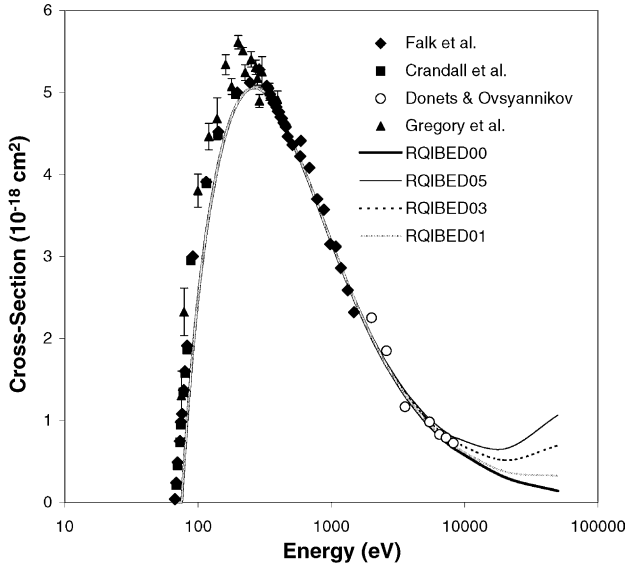

Fig. 1. The EI ionization cross-sections of N^{3+}, summed over all orbits, calculated in the RQIBED model for different values of the parameter d_2 with $d_1 = 0.0$ fixed, are compared with the experimental data from Falk et al. [64], Donets and Ovsyannikov [66], Crandall et al. [67] and Gregory et al. [68]. The heavy solid, shaded, short-dashed and light solid curves are the RQIBED results using $d_2 = 0.0$, 0.01, 0.03 and 0.05, respectively.

3.1. Ionization of B^+

The siBED, QIBED and RQIBED predictions for B^+ are compared, in Fig. 2, with the experimental cross-section data [64], the findings from DWBX [52], the results from BRY [24] and the assessed data of Bell et al. [56]. The DWBX results follow closely the data and the predictions of QIBED or RQIBED. However, the agreement of the latter is much better.

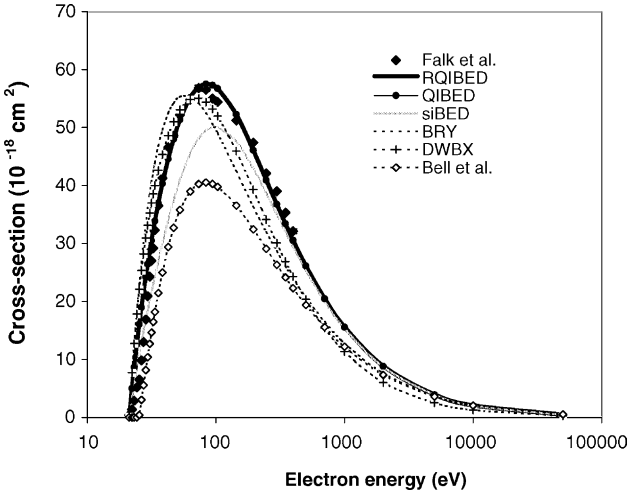

Fig. 2. The EI ionization cross-sections of B^+, summed over all orbits, as a function of incident energy. The calculated cross-sections from siBED (shaded curve), QIBED (curve with solid circles) and RQIBED (heavy solid curve) are compared with the experimental data of Falk et al. [64]. The dashed curve represents the results from the BRY model [24]. The dashed curve with pluses is from the DWBX calculations of Younger [52]. The dashed curve with the open diamonds are the assessed data of [56].

Throughout the entire energy range, the experimental data are reproduced excellently by the QIBED and RQIBED results, which are almost indistinguishable signifying the negligible contribution from the relativistic effect in the energy domain considered. The smallness of the relativistic effect is expected since the binding and the kinetic energies of the bound electron are not large. The siBED calculations underestimate the data substantially around the peak region. The difference between the results of siBED and QIBED is a clear signature of the significant contribution from the ionic correction incorporated in the latter.

Apart from the high energy tail, the BRY calculations give a poor fit to the data with the predicted peak position displaced towards the lower energies relative to the data peak. The DWBX results are somewhat better than those of BRY near the threshold and around the peak region, but surprisingly get worse at higher energies. The assessed data underestimate the experimental cross-sections at the peak, although agree in pattern with the latter.

3.2. Ionization of C^{2+}

In Fig. 3, we compare the calculated cross-sections from the siBED, QIBED and RQIBED models with the experimental data of Falk et al. [64], Woodruff et al. [65], Donets and Ovsyannikov [66]; the theoretical results of [51] from DCBX, [50] from NXDCB, and [52] from DWBX; our findings from BRY [24]; and the assessed data of [56]. As the data of [65] suggest that 40% contributions come from the metastable

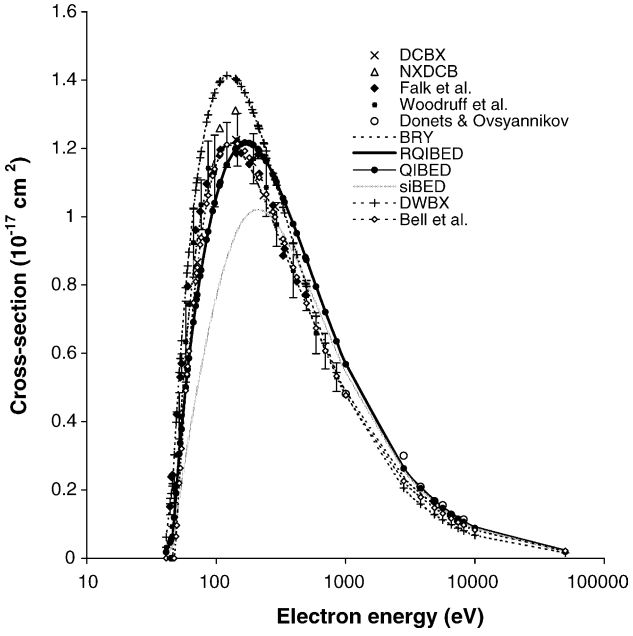

Fig. 3. The same as in Fig. 2 for C^{2+}. The calculated cross-sections from siBED (shaded curve), QIBED (curve with solid circles) and RQIBED (heavy solid curve) are compared to the experimental data of Falk et al. [64], Woodruff et al. [65], and Donets and Ovsyannikov [66].The open triangles and crosses are the theoretical results of NXDCB [50] and DCBX [51], respectively.

state, we have presented the calculations of DWBX, BRY, siBED, QIBED and RQIBED, with a mixture of the 60% and 40% contributions from the ground and metastable states, respectively.

Similar to the B^+ target, the predictions from the QIBED and RQIBED models are almost identical. The present results due to the siBED model underestimate the data in the low energy region, underscoring the importance of the ionic correction. Although the predicted peak position of the QIBED or RQIBED model is slightly shifted from the peak region of the data, there is a good agreement with both in the pattern and magnitudes of cross-sections between the calculations and experiments. In particular, there is an excellent agreement between the results of QIBED and experiments at low and high energies. The BRY results produce the best fit to the experimental data. The cross-sections due to NXDCB [50], DCBX [51] and DWBX [52] and the data from [56] compare favorably with the findings of the either QIBED or RQIBED model.

3.3. Ionization of N^{3+}

Fig. 4 shows the comparison of the predicted cross-sections from siBED, QIBED and RIBED with the experimental data of Falk et al. [64], Donets and Ovsyannikov [66], Crandall et al. [67] and Gregory et al. [68]; the assessed data of Bell et al. [56]; the other theoretical results [50–53]; and the model calculations [24,55]. As is apparent from Fig. 4, QIBED and RQIBED produce an excellent fit to all the experimental data and agree fairly well with the recommended data of [56] up to the peak region. The QIBED or RQIBED model, however, underestimate the data beyond the peak region. The siBED predictions show a larger discrepancies with the data than the previous cases of B^+ and C^{2+}. This is a reflection of the increase in the ionic effect with the charge q of the target. However, at energies higher than about 1000 eV, the siBED calculations converge to the QIBED or RQIBED results. For this target, the relativistic effect still remains too meagre to show up any tangible difference in the QIBED and RQIBED results.

The MBED calculations describe the data well from the threshold to about the peak region, but underestimate the experimental data at energies beyond the peak. However, MBED shows good agreement with the other theoretical findings [50–53]. BRY produces worse results near the peak region but at higher energies it improves. At energies beyond the peak region, both the QIBED and the RQIBED models yield much better results than other calculations.

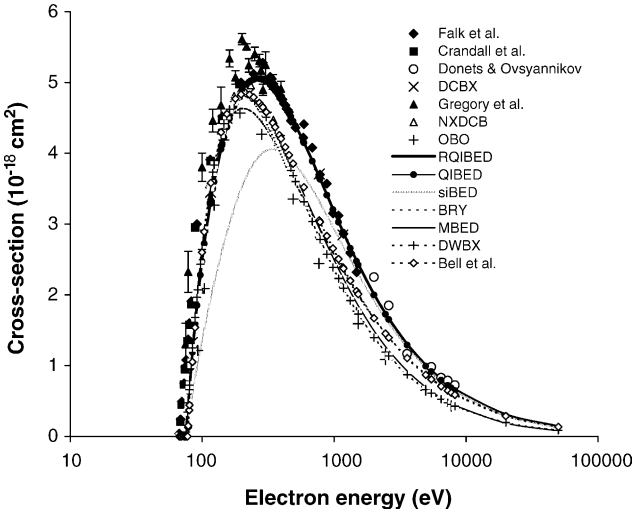

Fig. 4. The same as in Fig. 3 for N^{3+} excepting that the solid diamonds are the experimental data of Crandall et al. [67] and solid triangles are the data from Gregory et al. [68]. The pluses are the calculations from [53]. The thin solid curve represents the results from MBED [55].

3.4. Ionization of O^{4+}

In Fig. 5, we compare the siBED, QIBED and RQIBED results for O^{4+} with the experimental cross-sections of Falk et al. [64], Donets and Ovsyannikov [66], Crandall et al. [67], and Ganas and Green [69]; the assessed data of Bell et al. [56]; the results of DCBX [51] and DWBX [52] quantal calculations; and the predictions from BRY [24] and MBED [55].

The QIBED and RQIBED results, which are almost indistinguishable even for this target, produce by far the best description of data relative to the other calculations. The former two models, however, fail to reproduce the structure of the data near the peak region. The discrepancy between the siBED calculations and the data up to about 1000 eV justifies the ionic correction in the QIBED and RQIBED models. The

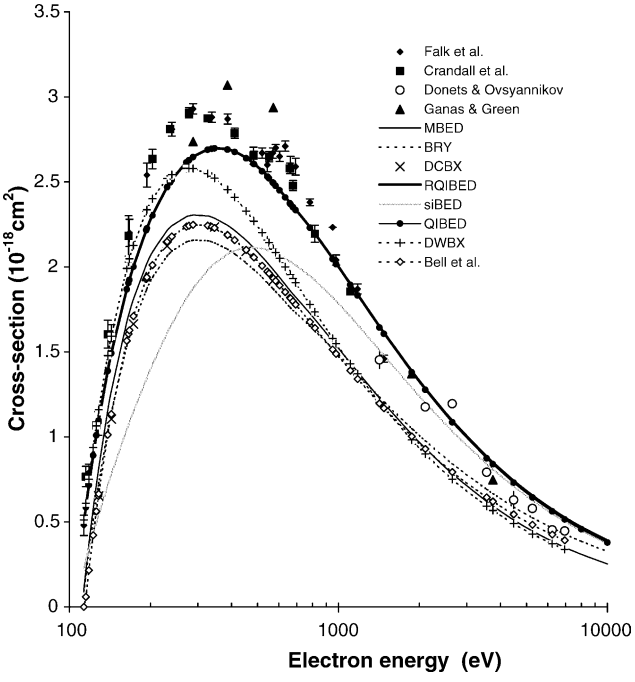

Fig. 5. The same as in Fig. 3 for O^{4+} excepting that the solid triangles are the data of Ganas and Green [69].

kinetic and binding energies are not yet sufficiently high to reflect the relativistic effect from the RQIBED findings. The MBED predictions, although close to those of [51] and BRY, underestimate the experimental data in most of the energy region. However, BRY reproduces the data of [66] at the high energy end. DWBX [52], on the other hand, reproduces the data from threshold to the peak region well, but underestimate the experimental cross-sections beyond the peak region. The assessed data [56] seem to underestimate all the available experimental data.

The figure also shows an enhancement of the cross-sections at around 550 eV due to the contribution of the excitation-autoionization (EA) [64]. A contribution from the metastable state of the target may also be possible. These two factors may cause discrepancy as neither QIBED nor RQIBED has provisions for these physical aspects.

3.5. Ionization of Ne^{6+}

In Fig. 6, the siBED, QIBED and RQIBED results are compared with the experimental cross-sections of Donets and Ovsyannikov [66], Duponchelle et al. [70], and Bannister [71]; the model calculations from BRY [24] and MBED [55]; and the quantal results of DWBARM [16] and DCBX [51]. The MBED results agree very well with all experimental data except the data of [66] at higher energies. QIBED and RQiBED, which generate almost identical results, show excellent fit to the data up to the peak region and at higher energies, but disagree with the data of [70] slightly beyond the peak region. The siBED calculations show a larger discrepancies with the data and the findings of either QIBED or RQIBED, suggesting the increasing ionic effect with the charge q of the target.

The DWBARM calculations of [16], which includes the indirect EA process, yield good agreement with all experimental data, except the data of [66]. A comparison of results due to the MBED model and the DWBARM theory shows that the contribution from EA is not significant, in conformity with the earlier observation of Uddin et al. [55]. The discrepancies between the data of [66] and those of [70] in the overlapping region is noticeable.

3.6. Ionization of Fe^{22+}

To the best of our knowledge, the experimental data on Fe^{22+} are not available. The motivation of using this target with an appreciable value of $q = 22$ is to study the role of relativistic effects. We compare, in Fig. 7, the predicted cross-sections from QIBED and RQIBED with the findings from the siBED, BRY, and MBED models; and the results due to the DCBX [51] and DWBX [52] methods.

The difference between the QIBED and RQIBED results shows the effect of the relativistic correction. Except at high energies, the siBED results greatly underestimate other theoretical cross-sections. At higher energies the DCBX and DWBX results are very similar but fall off more rapidly than the QIBED and RQIBED values. We have observed the similar trend in O^{4+} (Fig. 5) and Ne^{6+} (Fig. 6). The rate of fall of other theoretical cross-sections with energy may be partly due to the fact that the associated methods are non-relativistic and the Born cross-sections may not be adequate at relativistic energies. The rising tendency of the predicted cross-sections

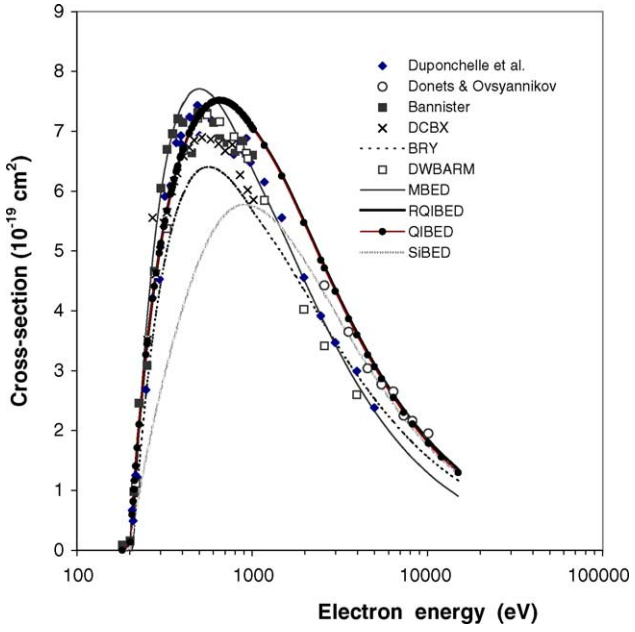

Fig. 6. The same as in Fig. 3 for Ne^{6+} excepting that the solid diamonds and solid squares are the data from Duponchelle et al. [70] and Bannister [71]. The open diamonds are the DWBARM results from [16].

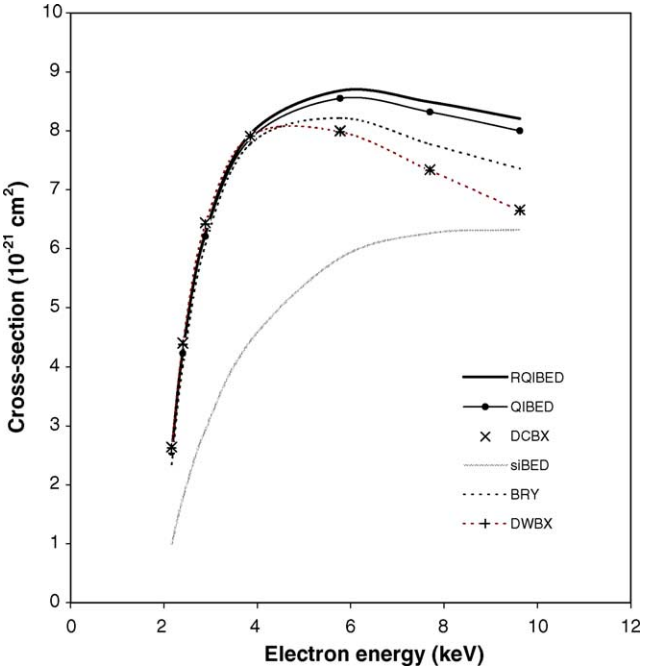

Fig. 7. The same as in Fig. 2 for Fe^{22+}. The crosses are the DCBX calculations [51].

with siBED is due to the absence of the ionic factor in its structure, which becomes prominent at the low energies and decreases with the increase of the incident energies as expected.

3.7. Ionization of U^{88+}

There are yet no experimental data on U^{88+}. Fig. 8 compares the calculated 2s-orbit ionization cross-sections from our QIBED and RQIBED models with the DWBX [52] and RDWBA [54] results.

In the QIBED and RQIBED models, the EI ionization cross-sections are determined by the ionization potential I and kinetic energy U of the bound electron in addition to the incident energy T. It is to be noted that $I(2s) = 32.46$ keV and $U(2s) = 27.67$ keV for U^{88+} closely resemble to $I(1s) = 29.38$ keV and $U(1s) = 33.31$ keV for Sn. Thus the EI cross-sections for U^{88+} in the 2s-orbit should be close to those for the K-shell ionizations of Sn. The comparison of the predicted results in Fig. 8 with the experimental data of Rester and Dance [72] for Sn shows that RQIBED describes the data well. The RDWBA calculations fall off with energy faster than the data, while DWBX and QIBED greatly underestimate the results of RQIBED and RDWBA. The discrepancy between the QIBED and RQIBED results relay the importance of the relativistic effect which is significantly large for this target.

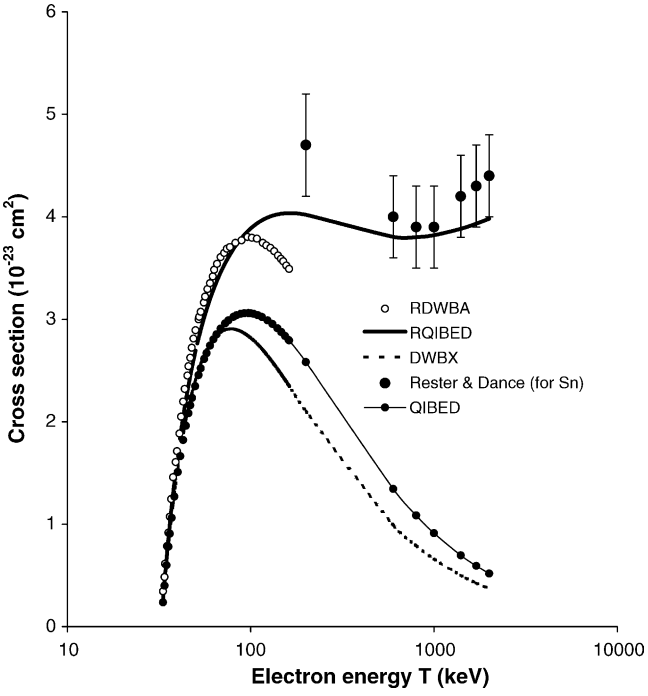

Fig. 8. The EI ionization cross-section of U^{88+} for the 2s orbit. The RQIBED predictions in solid curve, QIBED results in thin solid curve with solid dots, DWBX calculations of [52], in broken curve and RDWBA results of [54] in open circles are compared with the experimental data of [72] for K-shell ionization of Sn (see text for explanation).

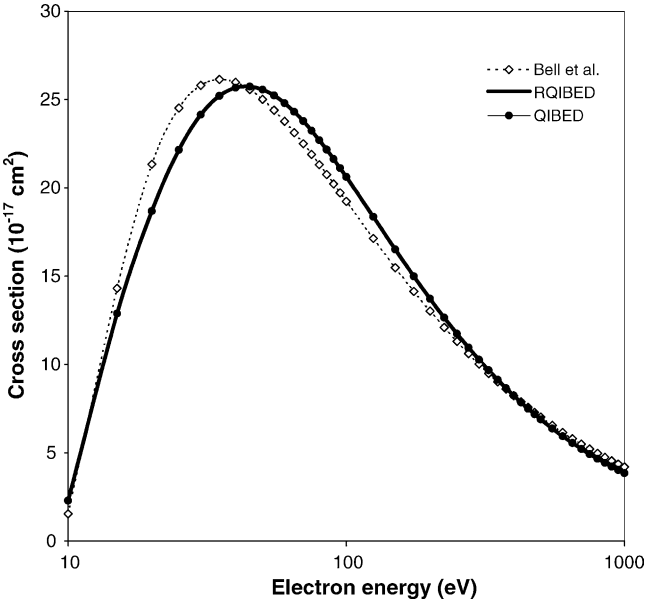

Fig. 9. The EI ionization cross-sections of Be. The calculated cross-sections from RQIBED (heavy solid curve) and QIBED (curve with solid circles) are compared with the assessed data (in broken curve with open diamonds) of Bell et al. [56].

3.8. Ionization of Be

To the best of our knowledge, no experimental or theoretical data, other than the assessed cross-sections of Bell et al. [56], are available on the atomic Be. The predictions of the RQIBED model are compared with the assessed data in Fig. 9. The results due to Bell et al. compare close to the data except for a narrow region beyond the peak region.

4. Conclusions

The present work reports the performance of the siBED model [45] along with its extensions, the QIBED and RQIBED models [55] on the neutral Be atom and the ions in the Be isoelectronic sequence e.g. B^+, C^{2+}, N^{3+}, O^{4+}, Ne^{6+} and U^{88+}. Replacing the Bethe part in the BED model [35] by the Born cross-section term with the two parameters in the siBED model [45], seems to bear a far reaching consequence. The identical values, of $d_1 = d_2 = 0.0$ for the Be-like targets in the present work and for the K-shell ionization [49], suggest that the generic values of the two parameters in the QIBED and RQIBED models are amply dependent on the electronic configuration of the targets. Using the same set of values for the parameters d_1 and d_2 in this study, it is observed that the QIBED and RQIBED models produce almost similar results which describe satisfactorily the data of these ions and the assessed data of Be in the non-relativistic domain. In the relativistic region, the difference between the results of QIBED and RQIBED begins to manifest for Fe^{22+} (Fig. 7) and become significantly large for U^{88+} (Fig. 8). The RQIBED results, with the same values of d_1 and d_2, for the ionization cross-section for the 2s-orbit of U^{88+} agree very

well with the experimental data for the K-shell ionization for Sn.

In the present study, the generic values of the two parameters, $d_1 = d_2 = 0.0$, provide the best fits to the data of all Be-like targets. The same values are found good for the EI K-shell ionization investigation we reported recently [49]. This is expected as, in both cases, the ionization takes place from the filled s-orbit. If it is found possible to obtain generic values for other isoelectronic sequences, then RQIBED will be a lucrative simple model, the practitioners are looking for.

Acknowledgement

The authors are thankful to Professor F. Bary Malik of Southern Illinois University at Carbondale, USA for valuable comments and constant encouragements.

References

[1] A.S. Kadyrov, A.M. Mukhamedzhanov, A.T. Stelbovics, I. Bray, Phys. Rev. Lett. 91 (2003) 253202.
[2] A.S. Kadyrov, A.M. Mukhamedzhanov, A.T. Stelbovics, Phys. Rev. A 67 (2003) 024702.
[3] P.L. Bartlett, A.T. Stelbovics, I. Bray, Phys. Rev. A 68 (2003) 030701.
[4] T.N. Rescigno, M. Baertschy, D. Byrum, C.W. McCurdy, Phys. Rev. A 55 (1997) 4253.
[5] F. Robicheaux, M.S. Pindzola, D.R. Plante, Phys. Rev. A 55 (1997) 3573.
[6] M. Baertschy, T.N. Rescigno, W.A. Isaacs, X. Li, C.W. McCurdy, Phys. Rev. A 63 (2001) 022712.
[7] Y. Attaoutti, P. Defrance, A. Makhaute, C.J. Joachain, Physica Scripta 43 (1991) 578.
[8] T.-Y. Kuo, K.-N. Huang, Phys. Rev. A 64 (1995) 032710.
[9] S.M. Younger, J. Quant. Spectrosc. Radiat. Transfer 26 (1981) 329.
[10] S.M. Younger, Phys. Rev. A 26 (1982) 3177.
[11] I. Bray, A.T. Stelbovics, Phys. Rev. Lett. 69 (1992) 53.
[12] I. Bray, A.T. Stelbovics, Phys. Rev. Lett. 70 (1993) 746.
[13] I. Bray, J. Phys. B 28 (1995) L247.
[14] K. Bartschat, E.T. Hudson, M.P. Scott, P.G. Burke, V.M. Burke, J. Phys. B 29 (1996) 115.
[15] K. Bartschat, E.T. Hudson, M.P. Scott, P.G. Burke, V.M. Burke, Phys. Rev. A 54 (1996) R998.
[16] K. Laghdas, R.H.G. Reid, C.J. Joachain, P.G. Burke, J. Phys. B 32 (1996) 1439.
[17] D.M. Mitnik, M.S. Pindzola, D.C. Griffin, N.R. Badnell, J. Phys. B 32 (1999) L479.
[18] M.P. Scott, H. Teng, P.G. Burke, J. Phys. B 33 (2000) L63.
[19] A. Riahi, K. Laghdas, R.H.G. Reid, S. Rachafi, C.J. Joachain, P. Defrance, J. Phys. B 34 (2001) 175.
[20] J.J. Thomson, Phil. Mag. 23 (1912) 449.
[21] W. Lotz, Z. Phys. 216 (1968) 241.
[22] W. Lotz, Z. Phys. 232 (1970) 101.
[23] M. Gryzinski, Phys. Rev. 138 (1965) 336.
[24] V.A. Bernshtam, Y.V. Ralchenko, Y. Maron, J. Phys. B 33 (2000) 5025.
[25] H. Deutsch, T.D. Märk, Int. J. Mass Spectrom. Ion Process. 79 (1987) R1.
[26] H. Deutsch, K. Becker, S. Matt, T.D. Märk, Int. J. Mass Spectrom. 197 (2000) 37.
[27] D. Margreiter, H. Deutsch, T.D. Märk, Int. J. Mass Spectrom. Ion Process. 139 (1994) 127.
[28] H. Deutsch, K. Becker, T.D. Märk, Contr. Plasma Phys. 35 (1995) 421.
[29] H. Deutsch, K. Becker, T.D. Märk, Int. J. Mass Spectrom. 177 (1998) 47.
[30] H. Deutsch, K. Becker, T.D. Märk, Int. J. Mass Spectrom. 185 (1999) 319.
[31] H. Deutsch, K. Becker, P. Defrance, U. Onthong, R. Parajuli, M. Probst, S. Matt, T.D. Märk, J. Phys. B 35 (2002) L65.
[32] H. Deutsch, K. Becker, B. Gstir, T.D. Märk, Int. J. Mass Spectrom. 213 (2002) 5.
[33] S.M. Younger, T.D. Märk, in: T.D. Märk, G.H. Dunn (Eds.), Electron Impact Ionization, Springer-Verlag, Berlin, 1985, p. 24.
[34] D.L. Moores, K.J. Reed, Adv. Atom. Mol. Opt. Phys. 34 (1994) 301.
[35] Y.-K. Kim, M.E. Rudd, Phys. Rev. A 50 (1994) 3954.
[36] J.M. Rost, J. Phys. B 28 (1995) 3003.
[37] V. Saksena, M.S. Kushwaha, S.P. Khare, Physica B 23 (1997) 201.
[38] S.P. Khare, M.K. Sharma, S. Tomar, J. Phys. B 32 (1999) 3147.
[39] M.A. Uddin, A.K. Basak, B.C. Saha, Int. J. Quant. Chem. 100 (2004) 184.
[40] W. Hwang, Y.-K. Kim, M.E. Rudd, J. Chem. Phys. 104 (1996) 2956.
[41] Y.-K. Kim, W. Hwang, N.M. Weinberger, M.A. Ali, M.E. Rudd, J. Chem. Phys. 106 (1997) 1026.
[42] Y.-K. Kim, J. Migdalek, W. Siegel, J. Bieron, Phys. Rev. A 57 (1998) 246.
[43] Y.-K. Kim, P.M. Stone, Phys. Rev. A 64 (2001) 052707.
[44] A. Burgess, I.C. Parceival, Adv. Atom. Mol. Phys. 4 (1968) 109.
[45] W.M. Huo, Phys. Rev. A 64 (2001) 042719.
[46] M.A. Uddin, A.K.F. Haque, A.K. Basak, B.C. Saha, Phys. Rev. A 70 (2004) 032706.
[47] K.K. Irikura, Y.-K. Kim, Res. Natl. Inst. Stand. Technol. 107 (2002) 63.
[48] Y.-K. Kim, Phys. Essays 13 (2000) 473.
[49] M.A. Uddin, A.K.F. Haque, M.M. Billah, A.K. Basak, K.R. Karim, B.C. Saha, Phys. Rev. A 71 (2005) 032715.
[50] D.L. Moores, J. Phys. B 11 (1978) L403.
[51] H. Jacubowicz, D.L. Moores, J. Phys. B 14 (1981) 3733.
[52] S.M. Younger, Phys. Rev. A 24 (1981) 1278.
[53] I.E. McCarthy, A.T. Stelbovics, Phys. Rev. A 28 (1983) 1322.
[54] D.L. Moores, K.J. Reed, J. Phys. B 28 (1995) 4861.
[55] M.A. Uddin, A.K. Basak, A.K.M.A. Islam, F.B. Malik, J. Phys. B 37 (2004) 1909.
[56] K.L. Bell, H.B. Gilbody, J.G. Hughes, A.E. Kingston, F.J. Smith, J. Phys. Chem. Ref. Data 12 (1983) 891.
[57] M. Inokuti, Rev. Mod. Phys. 43 (1971) 297.
[58] E. Casnati, A. Tartari, C. Baraldi, J. Phys. B 15 (1982) 155.
[59] C. Hombourger, J. Phys. B 31 (1998) 3693.
[60] J.P. Desclaux, Atom. Data Nucl. Data Tables 12 (1973) 325.
[61] M.Y. Amusia, L.V. Chernysheva, Computations of Atomic Processes, Institute of Physics Publishing, Bristol, 1997.
[62] F. Scheid, Numerical Analysis, Schaums Outline Series, McGraw-Hill, Singapore, 1988.
[63] F. James, M. Roos, Comput. Phys. Commun. 10 (1975) 343.
[64] R.A. Falk, G. Stefani, R. Camilloni, G.H. Dunn, D.C. Gregory, D.H. Crandall, Phys. Rev. A 28 (1983) 91.
[65] P.R. Woodruff, M.-C. Hublet, M.F.A. Harrison, J. Phys. B 11 (1978) 305.
[66] E.D. Donets, V.P. Ovsyannikov, Sov. Phys. JEEP 53 (1981) 466.
[67] D.H. Crandall, R.A. Phaneuf, B.E. Hasselquist, D.C. Gregory, J. Phys. B 12 (1979) L249.
[68] D.C. Gregory, D.H. Crandall, R.A. Phaneuf, A.M. Howald, G.H. Dunn, R.A. Falk, D.W. Mueller, T.J. Morgon, ORNL/TM (1985) 9501.
[69] P.S. Ganas, A.E.S. Green, Quant. Spectrosc. Radiat. Transfer 25 (1981) 265.
[70] M. Duponchelle, M. Khoulid, E.M. Onalim, H. Zhany, P. Defrance, J. Phys. B 30 (1997) 729.
[71] M.E. Bannister, Phys. Rev. A 54 (1996) 1435.
[72] D.H. Rester, W.E. Dance, Phys. Rev. 152 (1966) 1.